above. Cell viability was measured by the tetrazolium salt-based proliferation assay (WST assay; Wako Chemicals, Osaka, Japan). Briefly, treated cells (5×10^4 cells/well) in 96-well plates (Corning) were incubated overnight. After incubation for 24 h, the medium was changed to a new medium containing 10% WST-8 reagents. After incubation for 1 h, the absorbance of the formazan product formed was detected at 450 nm in a 96-well spectrophotometric plate reader (SpectraMax 190; Molecular Devices, Sunnyvale, CA, USA). Cell viability was measured and compared with that of the nontreated control cells. *In vitro* tests were conducted in triplicate.

■ Luciferase activity assay *in vitro*

Luciferase activity was analyzed using the Pica Gene luciferase assay system (Toyo Ink, Tokyo, Japan). Cells were harvested by centrifugation at 2000 rpm for 5 min at 4°C and lyzed by the addition of 5 µl of the lysis buffer. The lysate was freezed–thawed in liquid nitrogen. Thereafter, the luciferase activity of 5 ng of protein was quantified.

■ siRNA

The sequence data of siRNA targeted to the luciferase gene and nonspecific siRNA are as follows: luciferase siRNA: 5′-sense strand, 5′-ACAUCACUU ACGCUGAGUACUUCGAAG-3′ and 5′-antisense strand, 5′-UCGAAGUACUCA-GCGUAAGUGAUGUAU-3′ (Hokkaido System Science, Sapporo, Japan); nonspecific siRNA: 5′-sense strand, 5′-CCCUCUAG-UCUAGCGAGAUAAUUCAAG-3′ and 5′-antisense strand, 5′-UGAAUUAUCU-CGCUAGACUAGAGGGAU-3′ (iGENE, Tokyo, Japan). The siRNA was diluted to 100 pmol/µl (µM) by DNase, RNase-free water (GIBCO).

■ siRNA transfection using the optimum conditions of UBL *in vitro* & *in vivo*

siRNA transfection was conducted using the optimum conditions according to the simulation experiment described earlier. RT-112^{Luc} cells (6.0×10^5), siRNA (500 nM, final concentration) and the BL (0.2 mg/ml, final concentration) were plated into a 48-well plate. Then the well was irradiated by US at 1 W/cm^2 for 10 s at 30 s after the addition of the BL. These conditions demonstrated the best transfection efficiency under the condition that more than 60% of cells compared with the nontreated control survive.

■ *In vivo* UBL

RT-112^{Luc} cells (5×10^6 cells/100 µl) were injected subcutaneously in the left back skin of 6-week-old female BALB-c nu/nu mice (SLC, Shizuoka, Japan) (day -5). At 3 and 5 days after tumor implantation (day -2, 0), luciferase activity was measured as count per minute (cpm) using Photon Imager (Biospace, Paris, France). Mice bearing an RT-112^{Luc} tumor (tumor size: 5 mm) were divided into groups consisting of four mice and were treated using UBL and luciferase siRNA or nonspecific siRNA. The mice were then anesthetized with 2,2,2-tribromoethanol (250 mg/kg; Wako) and 2-methyl-2-butanol (250 µl/kg; Wako). Luciferase siRNA (600 pmol) in 80 µl of PBS and 20 µl of the BL were mixed and immediately injected into the tumor. A total of 30 s after intratumor injection of the mixture of the BL and siRNA, the mice were exposed to US irradiation (intensity: 1 W/cm^2, Duty Ratio: 50%, exposure time: 10 s). Intratumor administration of nonspecific siRNA was performed in the same manner as that for the control. After the treatment, luciferase activity was measured as cpm using Photon Imager® until 3 days after the treatment.

All animal procedures were performed in compliance with the Guidelines for the Care and Use of Experimental Animals of the National Cancer Center, Japan; these guidelines meet the ethical standards required by law and also comply with the guidelines for the use of experimental animals in Japan.

■ Histological toxicity of UBL *in vivo*

The PBS (80 µl) and BL (20 µl) were mixed and immediately injected into the left back skin of 6-week-old female BALB-c nu/nu mice. After 30 s from the injection of the BL, these mice were exposed to US irradiation (intensity: 0, 1, 2, 3 or 4 W/cm^2, duty ratio: 50%, exposure time: 10 s). These treatments were conducted three times (days 0, 2 AND 4). Skin lesions were collected 24 h after the last US irradiation and fixed in 3.7% formaldehyde/PBS. Paraffin-embedded tissue was cut (3 µm thick) and deparaffinized, followed by staining with hematoxylin and eosin. Inflammation was scored by a pathologist using an inflammation scale from – to + +, with – indicating no inflammation, + denoting mild inflammation predominantly infiltrated with neutrophils and ++ indicating active inflammation infiltrated with neutrophils and lymphocytes.

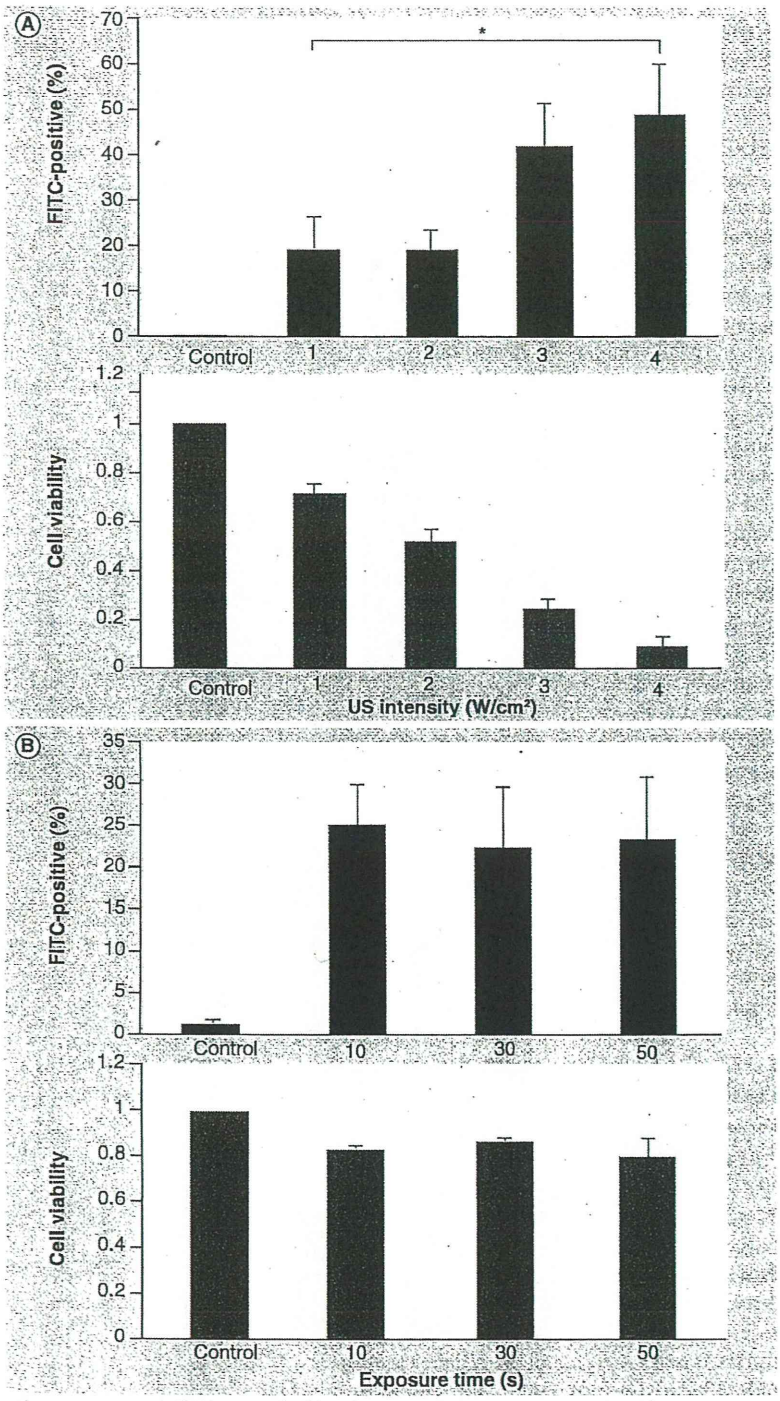

Figure 1. Determination of optimum ultrasound-mediated destruction of bubble liposome conditions. (A) Effects of US intensity on the rate of FITC-positive cells and cell viability in ultrasound-mediated destruction of bubble liposome (UBL). There was a significant difference in the rate of FITC-positive cells between 1–4 W/cm² intensities. **(B)** Effects of US exposure times on the rate of FITC-positive cells and cell viability in UBL. There were no significant differences in the rate of FITC-positive cells and cell viability between all groups.
*$p < 0.05$.
FITC: Fluorescein isothiocyanate; US: Ultrasound.

■ Statistical analysis

Statistical analysis was performed using Microsoft Excel (Microsoft Corporation, WA, USA). Values are expressed as mean ± standard deviation. Differences between groups were analyzed using two-sided Student's *t*-test. p-values lower than 0.05 were considered significant.

Results

■ Optimum conditions of UBL *in vitro*

US intensity

The effects of US intensity on FITC-positive cell rate and cell viability are shown in **Figure 1A**. The FITC-positive cell rates at 1, 2, 3 and 4 W/cm² US intensity were 19.71 ± 7.18% (mean ± SD), 19.91 ± 3.99, 42.52 ± 9.66 and 49.30 ± 11.55%, respectively. The rate of FITC-positive cells increased in an intensity-dependent manner. There was a significant difference in the FITC-positive cell rate between the UBL using 1 W/cm² US and that using 4 W/cm² US. The cell viabilities at 1, 2, 3 and 4 W/cm² US intensity were 70.40 ± 4.21, 50.42 ± 5.11, 22.76 ± 4.19 and 8.14 ± 3.22%, respectively. Conversely, cell viability decreased in an intensity-dependent manner.

■ US exposure time

The effects of US exposure time on FITC-positive cell rate and cell viability are shown in **Figure 1B**. The FITC-positive cell rates using 10, 30 and 50 s of US exposure time were 24.68 ± 5.14, 21.71 ± 7.72 and 22.98 ± 7.84%, respectively, with no significant difference between the three groups. The cell viabilities using 10, 30 and 50 s of US exposure time were 85.09 ± 2.02, 89.13 ± 1.31 and 82.81 ± 9.81, respectively.

■ BL concentration

The effects of BL concentration on FITC-positive cell rate and cell viability are shown in **Figure 2A**. The FITC-positive cell rates using 0.1, 0.2 and 0.3 mg/ml BL were 11.45 ± 4.04, 26.61 ± 5.72 and 19.54 ± 2.22%, respectively, with significant differences between 0.2 and 0.1 or 0.3 mg/ml. The cell viabilities using 0.1, 0.2 and 0.3 mg/ml BL were 90.24 ± 8.40, 72.32 ± 10.67 and 51.05 ± 12.09%, respectively.

■ Interval from BL addition to US exposure

The effects of interval from the BL addition to US exposure on FITC-positive cell rate and cell viability are shown in **Figure 2B**. The FITC-positive cell rates 15, 30, 60 and 300 s after the BL addition were 10.46 ± 0.03, 15.92 ± 3.05, 12.56 ± 2.40 and 5.27 ± 1.49%, respectively,

with significant differences between 30 and 15 or 300 s. The cell viabilities 15, 30, 60 and 300 s after the BL addition were 68.46 ± 10.78, 64.96 ± 2.81, 78.87 ± 8.27 and 89.28 ± 6.72%, respectively.

Taken together, the results show that the optimum conditions of BL are as follows: US intensity: 1 W/cm^2; US exposure time: 10 s; BL concentration: 0.2 mg/ml and interval: 30 s.

■ siRNA transfection using UBL at the optimum conditions determined by the simulation experiment *in vitro* & *in vivo*

At 24 h after treatment with UBL and luciferase siRNA, luciferase activity was not significantly suppressed compared with treatment with UBL and nonspecific siRNA (**Figure 3**). However, 48 h after treatment with UBL and luciferase siRNA, luciferase activity was significantly suppressed compared with treatment with UBL and nonspecific siRNA ($p = 0.036$; **Figure 3**).

The luciferase activities of the two groups increased with time (**Figure 4A**). The luciferase activity in the group treated with UBL and luciferase siRNA tended to be suppressed compared with that in the group treated with UBL and nonspecific siRNA up to 3 days after treatment (**Figure 4B**). However, there was no significant difference between both groups (**Figure 4B**).

■ Histological toxicity of UBL

Ultrasound-irradiated skin showed no recognizable changes in appearance (data not shown). Pathological changes in the skin following US exposure were not confirmed in mice treated with 0, 1 or 2 W/cm^2 US (**Figure 5**). Neutrophilic infiltration was, however, confirmed in mice treated with 3 or 4 W/cm^2 US (**Figure 5**; arrow).

Discussion & conclusion

This study mainly demonstrated the optimum conditions of UBL for siRNA transfection to the human bladder cell line RT-112^{Luc}. Gene or nucleic acid transfer utilizing UBL is expected to be a novel and promising strategy to overcome the severe adverse effects of intravesical administration of BCG currently used in clinics [2]. However, sonoporation has adverse effects according to the US energy and other conditions when it is used [28–30]. We therefore initially conducted several simulation experiments utilizing FITC-dextran transfer to cells as a surrogate marker to determine the best conditions of UBL with least toxic and maximum transfer effects. The molecular weight (MW) of FITC-dextran used in the present experiments

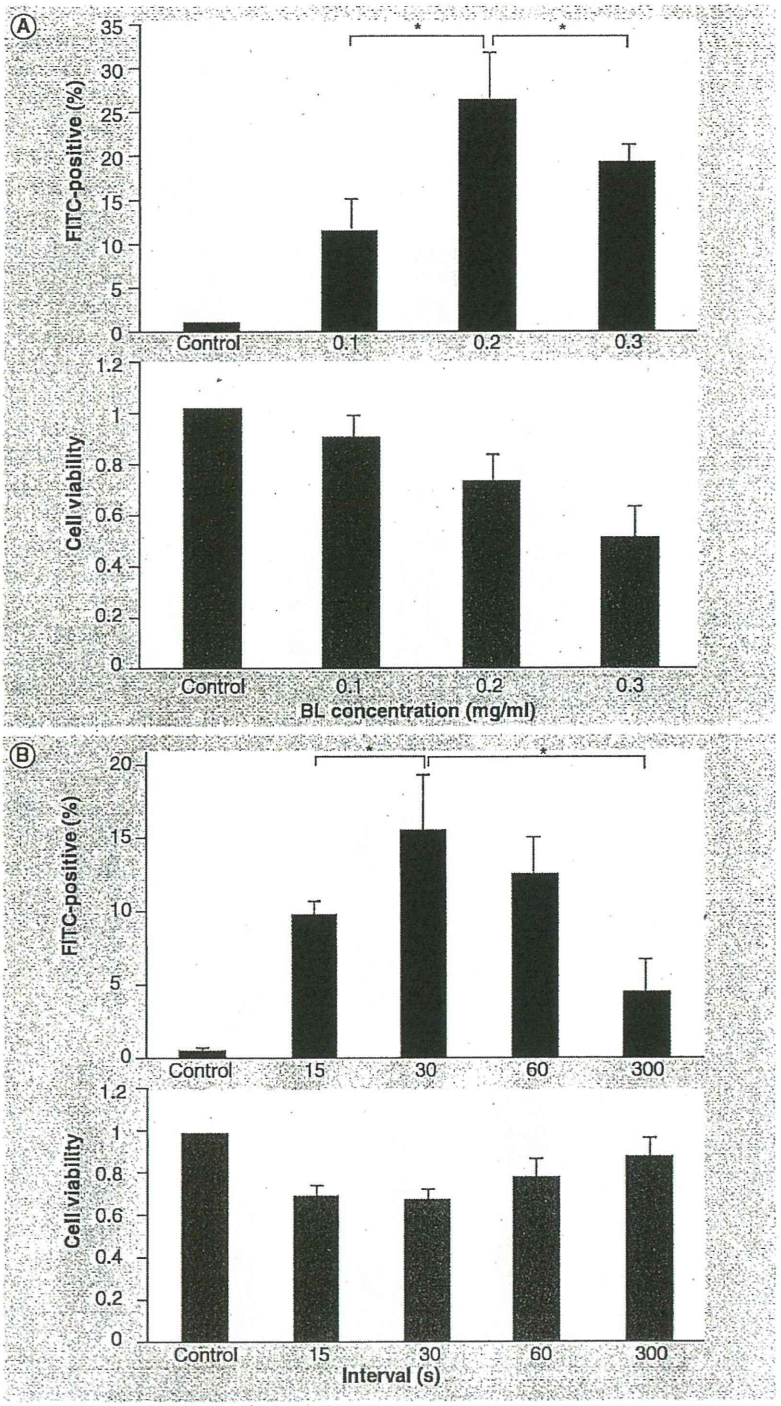

Figure 2. Determination of optimum ultrasound-mediated destruction of bubble liposome conditions. (A) Effects of bubble liposome (BL) concentration on the rate of FITC-positive cells and cell viability in ultrasound-mediated destruction of BL (UBL). There were significant differences in the rate of FITC-positive cells between 0.2 and 0.1 or 0.3 mg/ml. **(B)** Effects of intervals from BL addition to ultrasound exposure on the rate of FITC-positive cells and cell viability in UBL. There were significant differences in the rate of FITC-positive cells between 30 and 15 or 300 s. *$p < 0.05$.
FITC: Fluorescein isothiocyanate; BL: Bubble liposome.

was 10 kDa. Therefore, the pharmacodynamics of FITC-dextran according to the conditions of UBL may be extrapolated to that of siRNA, which has a MW of approximately 20 kDa.

Our preliminary study suggests that the BL should be used within 10 min after preparation, possibly due to its instability (data not shown). The optimum US intensity was further determined utilizing FITC-dextran transfer to cells. The ratio of FITC-positive cells increased but cell viability decreased in an intensity-dependent manner. These results indicate that higher gene transfer can be obtained by induction of microbubble collapse using higher US intensity, although such intensity was confirmed to cause cell toxicity. The optimum US intensity obtained *in vitro* appeared to be 1 W/cm^2 for siRNA transfer. These results are consistent with data published previously [17,18,31]. We also determined the optimum US exposure time by carrying out US irradiation to the cells for 10, 30 or 50 s. There were no significant differences in the rate of FITC-positive cells and cell viability in these three groups (**Figure 1B**). The present results were not in agreement with those of previous reports utilizing Optison™, wherein higher gene transfer was obtained with longer US exposure time [18,32]. Although the reason for these inconsistencies remain difficult to elucidate, it may be reasonable to conclude that a shorter US exposure time may be advantageous for US therapy in terms of exerting weaker adverse effects. In this study, the optimum US exposure time was determined to be 10 s. We also determined the optimum concentration of the BL for FITC-dextran transfer to cells. The ratio of FITC-positive cells in UBL with 0.2 mg/ml BL was the highest in the three groups. In addition, cell toxicity was higher when a higher concentration of the BL was used. These results are consistent with those of previous reports [20,32] and indicate a clear relationship between BL concentration and US effect. In this study, the optimum BL concentration was determined to be 0.2 mg/ml. Furthermore, we determined the optimum interval of the initiation of US exposure after the addition of the BL to the cell suspension. It was found that the optimum interval time was 30 s for the most effective FITC-dextran transfer to the cells. We speculated that the BL distributed throughout the solution 30 s after the addition of the BL and that the BL may be degraded afterward (**Figure 2B**). Taken together, several simulation experiments suggest the following optimum conditions of UBL: US intensity: 1 W/cm^2; US exposure time: 10 s; BL concentration: 0.2 mg/ml; interval: 30 s.

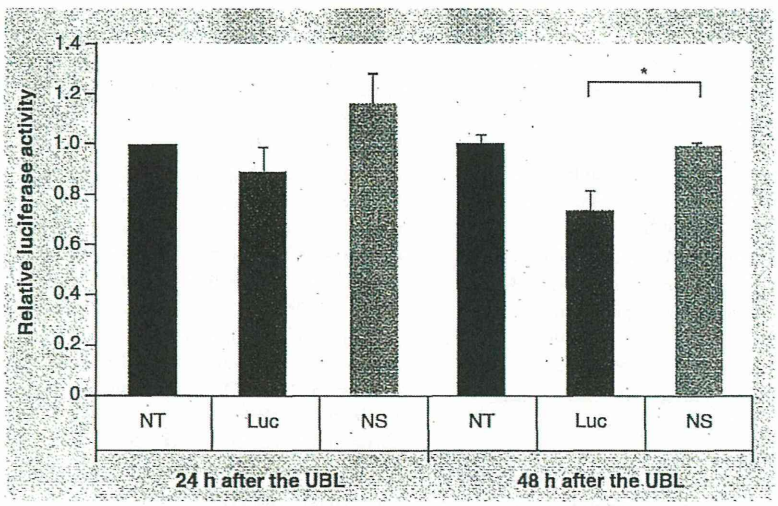

Figure 3. Suppression of luciferase activity by ultrasound-mediated destruction of bubble liposome with various siRNAs. Luciferase activity was affected by UBL with luciferase siRNA. There was a significant difference in the suppression of luciferase activity between UBL with luciferase siRNA and UBL with nonspecific siRNA 48 h after treatment.
*$p < 0.05$.
Luc: Luciferase siRNA; NS: Nonspecific siRNA; NT: Nontreatment; UBL: Ultrasound-mediated destruction of bubble liposome.

In addition, we found that UBL for luciferase siRNA transfer could suppress the expression of luciferase in RT-112^{Luc} cells (**Figure 3**). The results demonstrated that the optimal UBL conditions determined in this study could enable the transfer siRNA to cells.

The *in vivo* study demonstrated that within 48 h after UBL, luciferase activity with UBL for luciferase siRNA decreased compared with luciferase activity with UBL for nonspecific siRNA (**Figure 4**). However, this suppression disappeared 72 h after the treatment. This result is consistent with a previous report on sonoporation for the salivary gland, in which it was suggested that reduction of the RNAi effect was caused by siRNA degradation [15]. It was also previously suggested that the reduction of the RNAi effect in a dividing subcutaneous tumor might be caused by siRNA shortage due to tumor growth [3,33].

In the present study, UBL for siRNA transfer did not suppress luciferase activity significantly (**Figure 4B**). From the *in vivo* experiment, only a slight neutrophil infiltration as a result of inflammation was observed at 3 or 4 W/cm^2 US irradiation (**Figure 5**; arrow). Therefore, we speculate that higher US intensity may be used and this

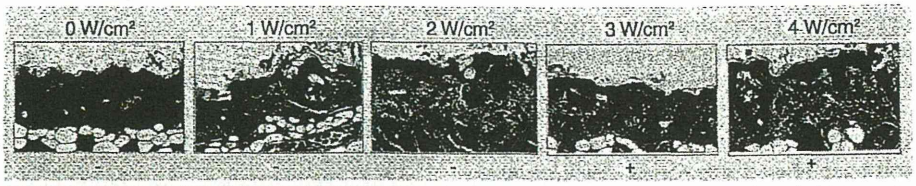

Figure 5. Adverse effects of ultrasound-mediated destruction of bubble liposome *in vivo*. Hematoxylin and eosin staining of skin (original magnification × 20). There were only slight infiltrations of neutrophils (arrow) at 3 or 4 W/cm² ultrasound exposure. Other adverse effects were not confirmed.

Financial & competing interests disclosure

This work was supported partly by a Grant-in-Aid from the 3rd Term Comprehensive Control Research for Cancer, Ministry of Health, Labor and Welfare (Yasuhiro Matsumura) and Scientific Research on Priority Areas from the Ministry of Education, Culture, Sports, Science and Technology (Yasuhiro Matsumura), and the Princess Takamatsu Cancer Research Fund (Yasuhiro Matsumura). The authors have no other relevant affiliations or financial involvement with any organization or entity with a financial interest in or financial conflict with the subject matter or materials discussed in the manuscript apart from those disclosed.

No writing assistance was utilized in the production of this manuscript.

Executive summary

- We initially conducted several simulation experiments utilizing fluorescein isothiocyanate (FITC)-dextran transfer to cells as a surrogate marker to determine the best conditions for ultrasound-mediated destruction of bubble liposome (UBL) with least toxic and maximum transfer effects.
- The ratio of FITC-positive cells increased in an intensity-dependent manner.
- The optimum conditions for UBL were determined as follows: ultrasound intensity: 1 W/cm²; US exposure time: 10 s; BL concentration: 0.2 mg/ml; interval: 30 s.
- The optimum UBL conditions determined in this study enabled siRNA transfer to cells.
- The *in vivo* study demonstrated that during the 48 h after UBL, luciferase activity with UBL for luciferase siRNA decreased compared with luciferase activity with UBL for nonspecific siRNA. However, this suppression disappeared 72 h after the treatment. UBL conditions must therefore be improved to obtain higher siRNA transfer.

Bibliography

Papers of special note have been highlighted as:
■■ of considerable interest

1 Gee J, Sabichi AL Grossman HB. Chemoprevention of superficial bladder cancer. *Crit. Rev. Oncol. Hematol.* 43(3), 277–286 (2002).

2 Shelley MD, Kynaston H, Court J *et al.* A systematic review of intravesical bacillus Calmette–Guerin plus transurethral resection vs transurethral resection alone in Ta and T1 bladder cancer. *BJU Int.* 88(3), 209–216 (2001).

3 Fire A, Xu S, Montgomery MK, Kostas SA, Driver SE, Mello CC. Potent and specific genetic interference by double-stranded RNA in *Caenorhabditis elegans*. *Nature* 391(6669), 806–811 (1998).

4 Elbashir SM, Harborth J, Lendeckel W, Yalcin A, Weber K, Tuschl T. Duplexes of 21-nucleotide RNAs mediate RNA interference in cultured mammalian cells. *Nature* 411(6836), 494–498 (2001).

5 Song E, Lee SK, Wang J *et al.* RNA interference targeting Fas protects mice from fulminant hepatitis. *Nat. Med.* 9(3), 347–351 (2003).

6 Nogawa M, Yuasa T, Kimura S *et al.* Intravesical administration of small interfering RNA targeting PLK-1 successfully prevents the growth of bladder cancer. *J. Clin. Invest.* 115(4), 978–985 (2005).

7 Ohta S, Suzuki K, Tachibana K, Yamada G. Microbubble-enhanced sonoporation: efficient gene transduction technique for chick embryos. *Genesis* 37(2), 91–101 (2003).

8 Ohta S, Suzuki K, Ogino Y *et al.* Gene transduction by sonoporation. *Dev. Growth. Differ.* 50(6), 517–520 (2008).

9 Michel MS, Erben P, Trojan L *et al.* Acoustic energy: a new transfection method for cancer of the prostate, cancer of the bladder and benign kidney cells. *Anticancer Res.* 24(4), 2303–2308 (2004).

10 Shohet RV, Chen S, Zhou YT *et al.* Echocardiographic destruction of albumin microbubbles directs gene delivery to the myocardium. *Circulation* 101(22), 2554–2556 (2000).

11 Sonoda S, Tachibana K, Uchino E *et al.* Gene transfer to corneal epithelium and keratocytes mediated by ultrasound with microbubbles. *Invest. Ophthalmol. Vis. Sci.* 47(2), 558–564 (2006).

12 Duvshani-Eshet M, Baruch L, Kesselman E, Shimoni E, Machluf M. Therapeutic ultrasound-mediated DNA to cell and nucleus: bioeffects revealed by confocal and atomic force microscopy. *Gene Ther.* 13(2), 163–172 (2006).

13 Tsunoda S, Mazda O, Oda Y *et al.* Sonoporation using microbubble BR14 promotes pDNA/siRNA transduction to murine heart. *Biochem. Biophys. Res. Commun.* 336(1), 118–127 (2005).

14 Saito M, Mazda O, Takahashi KA *et al.* Sonoporation mediated transduction of pDNA/siRNA into joint synovium *in vivo*. *J. Orthop. Res.* 25(10), 1308–1316 (2007).

■■ **Shows siRNA transfer to synovium by sonoporation *in vivo*. An effect of siRNA transfer to tissue by sonoporation *in vivo* was confirmed in this report.**

15 Sakai T, Kawaguchi M, Kosuge Y. siRNA-mediated gene silencing in the salivary gland using *in vivo* microbubble-enhanced sonoporation. *Oral. Dis.* 15(7), 505–511 (2009).

■■ Shows siRNA transfer to salivary gland by sonoporation *in vivo*. It also refers to a period of siRNA-induced gene silencing by sonoporation.

16 Suzuki J, Ogawa M, Takayama K *et al.*, Ultrasound-microbubble-mediated intercellular adhesion molecule-1 small interfering ribonucleic acid transfection attenuates neointimal formation after arterial injury in mice. *J. Am. Coll. Cardiol.* 55(9), 904–913.

17 Kinoshita M, Hynynen K. A novel method for the intracellular delivery of siRNA using microbubble-enhanced focused ultrasound. *Biochem. Biophys. Res. Commun.* 335(2), 393–399 (2005).

18 Kinoshita M, Hynynen K. Key factors that affect sonoporation efficiency in *in vitro* settings: the importance of standing wave in sonoporation. *Biochem. Biophys. Res. Commun.* 359(4), 860–865 (2007).

19 Newman CM, Bettinger T. Gene therapy progress and prospects: ultrasound for gene transfer. *Gene Ther.* 14(6), 465–475 (2007).

20 Li T, Tachibana K, Kuroki M. Gene transfer with echo-enhanced contrast agents: comparison between Albunex®, Optison™, and Levovist® in mice– initial results. *Radiology* 229(2), 423–428 (2003).

21 Taniyama Y, Tachibana K, Hiraoka K *et al.* Local delivery of plasmid DNA into rat carotid artery using ultrasound. *Circulation* 105(10), 1233–1239 (2002).

22 Suzuki R, Takizawa T, Negishi Y *et al.* Gene delivery by combination of novel liposomal bubbles with perfluoropropane and ultrasound. *J. Control. Release* 117(1), 130–136 (2007).

23 Suzuki R, Takizawa T, Negishi Y *et al.* Tumor specific ultrasound enhanced gene transfer *in vivo* with novel liposomal bubbles. *J. Control Release* 125(2), 137–144 (2008).

24 Suzuki R, Oda Y, Utoguchi N, Maruyama K. Progress in the development of ultrasound-mediated gene delivery systems utilizing nano- and microbubbles. DOI:10.1016/j.jconrel.2010.05.009 *J. Control Release* (2010) (Epub ahead of print).

25 Suzuki R, Namai E, Oda Y *et al.* Cancer gene therapy by IL-12 gene delivery using liposomal bubbles and tumoral ultrasound exposure. *J. Control Release* 142(2), 245–250 (2010).

26 Kodama T, Tomita N, Horie S *et al.* Morphological study of acoustic liposomes using transmission electron microscopy. *J. Electron Microsc. (Tokyo)* 59(3),187–196 (2010).

27 Negishi Y, Endo Y, Fukuyama T *et al.* Delivery of siRNA into the cytoplasm by liposomal bubbles and ultrasound. *J. Control Release* 132(2), 124–130 (2008).

28 Miller DL, Pislaru SV, Greenleaf JE. Sonoporation: mechanical DNA delivery by ultrasonic cavitation. *Somat. Cell Mol. Genet.* 27(1–6), 115–134 (2002).

29 Wei W, Zheng-zhong B, Yong-jie W, Qing-wu Z, Ya-lin M, Bioeffects of low-frequency ultrasonic gene delivery and safety on cell membrane permeability control. *J. Ultrasound Med.* 23(12), 1569–1582 (2004).

30 Koch S, Pohl P, Cobet U, Rainov NG. Ultrasound enhancement of liposome-mediated cell transfection is caused by cavitation effects. *Ultrasound Med. Biol.* 26(5), 897–903 (2000).

31 Li YS, Davidson E, Reid CN, McHale AP. Optimising ultrasound-mediated gene transfer (sonoporation) *in vitro* and prolonged expression of a transgene *in vivo*: potential applications for gene therapy of cancer. *Cancer Lett.* 273(1), 62–69 (2009).

32 Han YW, Ikegami A, Chung P, Zhang L, Deng CX. Sonoporation is an efficient tool for intracellular fluorescent dextran delivery and one-step double-crossover mutant construction in *Fusobacterium nucleatum*. *Appl. Environ. Microbiol.* 73(11), 3677–3683 (2007).

33 Bartlett DW, Davis ME. Insights into the kinetics of siRNA-mediated gene silencing from live-cell and live-animal bioluminescent imaging. *Nucleic Acids Res.* 34(1), 322–333 (2006).

34 Urban-Klein B, Werth S, Abuharbeid S, Czubayko F, Aigner A. RNAi-mediated gene-targeting through systemic application of polyethylenimine (PEI)-complexed siRNA *in vivo*. *Gene Ther.* 12(5), 461–466 (2005).

35 Soutschek J, Akinc A, Bramlage B *et al.* Therapeutic silencing of an endogenous gene by systemic administration of modified siRNAs. *Nature* 432(7014), 173–178 (2004).

36 Morrissey DV, Blanchard K, Shaw L *et al.* Activity of stabilized short interfering RNA in a mouse model of hepatitis B virus replication. *Hepatology* 41(6), 1349–1356 (2005).

37 Watanabe T, Shinohara N, Sazawa A *et al.* An improved intravesical model using human bladder cancer cell lines to optimize gene and other therapies. *Cancer Gene Ther.* 7(12), 1575–1580 (2000).

Advanced Drug Delivery Reviews 63 (2011) 184–192

Contents lists available at ScienceDirect

Advanced Drug Delivery Reviews

journal homepage: www.elsevier.com/locate/addr

Preclinical and clinical studies of NK012, an SN-38-incorporating polymeric micelles, which is designed based on EPR effect☆

Yasuhiro Matsumura *

Investigative Treatment Division, Research Center of Innovative Oncology, National Cancer Center Hospital East, 6-5-1, Kashiwanoha, Kashiwa, 277-8577, Japan

ARTICLE INFO

Article history:
Received 4 March 2010
Accepted 21 May 2010
Available online 31 May 2010

Keywords:
Drug delivery system
EPR effect
NK012
SN-38
Clinical trial

ABSTRACT

Polymeric micelles are ideally suited to exploit the EPR effect, and they have been used for the delivery of a range of anticancer drugs in preclinical and clinical studies.

NK012 is an SN-38-loaded polymeric micelle constructed in an aqueous milieu by the self-assembly of an amphiphilic block copolymer, PEG–PGlu(SN-38). The antitumor activity was evaluated in several orthotopic tumor models including glioma, renal cancer, stomach cancer, and pancreatic cancer. Two independent phase I clinical trials were conducted in Japan and the USA.

In the preclinical studies, it was demonstrated that NK012 exerted significantly more potent antitumor activity with no intestinal toxicity against various orthotopic human tumor xenografts than CPT-11. In clinical trials, predominant toxicity was neutropenia. Non-hematologic toxicity, especially diarrhea, was mostly Grade 1 or 2 during study treatments. Total 8 partial responses were obtained.

According to data of preclinical studies, NK012 showing enhanced distribution with prolonged SN-38 release may be ideal for cancer treatment because the antitumor activity of SN-38 is time dependent. Clinical studies showed that NK012 was well tolerated and had antitumor activity including partial responses and several occurrences of prolonged stable disease across a variety of advanced refractory cancers. Phase II studies are ongoing in patients with colorectal cancer in Japan and in patients with triple negative breast cancer and small cell lung cancer in the USA.

Contents

1. Preface

Irinotecan hydrochloride (CPT-11) is now approved for the treatment of various cancers including colorectal and lung cancers [1–4]. CPT-11 is a prodrug and is converted to SN-38, a biologically active metabolite of CPT-11, by carboxylesterases (CEs). SN-38 is an analog of the plant alkaloid camptothecin which targets DNA topoisomerase I. SN-38 exhibits up to 1000-fold more potent cytotoxic activity against various cancer cells in vitro than CPT-11 [5]. Although CPT-11 is converted to SN-38 in the liver and tumors, the metabolic conversion rate is less than 10% of the original volume of CPT-11 [6,7]. Moreover, the conversion of CPT-11 to SN-38 depends on the genetic inter-individual variability of CE activity [8]. Thus, further efficient use of SN-38 might be

☆ This review is part of the *Advanced Drug Delivery Reviews* theme issue on "EPR effect based drug design and clinical outlook for enhanced cancer chemotherapy".

* Tel.: +81 4 7134 6857; fax: +81 4 7134 6866.
E-mail address: yhmatsum@east.ncc.go.jp.

0169-409X/$ – see front matter © 2010 Elsevier B.V. All rights reserved.
doi:10.1016/j.addr.2010.05.008

Table 1
Example of other DDS of campto in oncolgy.

Name	Platform	Clinical stage
NKTR-102	PEG	Phase II
PEP02	Liposome	Phase II
CPX-1	Liposome	Phase II
IT-101	Cyclodextrin	Phase II
EZN-2208	Branch-PEG	Phase II
SN-2310	Vitamin E	Phase I
IHL-305	Liposome	Phase I

of great advantage and maybe attractive for cancer treatment. To date, many DDS of campto have been developed and some of them are now under clinical evaluation (Table 1). Polymeric micelle-based anticancer drugs were originally developed by Kataoka et al. in the late 1980s or early 1990s [9–11]. Polymeric micelles were expected to increase the accumulation of drugs in tumor tissues by utilizing the EPR effect [12]. Micelle system can also incorporate various kinds of drugs into their inner core with relatively high stability by chemical conjugation or physical entrapment. Also, the size of micelles can be controlled within the diameter range of 20 to 100 nm to ensure that they do not penetrate normal vessel walls. With this development, it is expected that the incidence of drug-induced side effects may be decreased owing to the reduced drug distribution in normal tissues. NK012 is an SN-38-loaded polymeric micelle constructed in an aqueous milieu by the self-assembly of an amphiphilic block copolymer, PEG–PGlu(SN-38) [13].

In this paper, preclinical and clinical studies of NK012 were reviewed.

2. Preparation of an SN-38 conjugated poly(ethylene glycol)–poly (glutamic acid) block copolymer [PEG–PGlu(SN-38)] for NK012 construction

PEG–PGlu(SN-38) was synthesized as follows: a poly(ethylene glycol)–poly(glutamic acid) block copolymer [PEG–PGlu] was prepared according to the technique reported previously [14,15]. SN-38 was covalently introduced into the poly(glutamic acid) [PGlu] segment by the condensation reaction between the carboxylic acid on PGlu and the phenol on SN-38 with 1,3-diisopropylcarbodiimide and N,N-dimethylaminopyridine at 26 °C. Consequently, the poly(glutamic acid) segment obtained sufficient hydrophobicity. Accordingly, NK012 was constructed with self-assembling PEG–PGlu(SN-38), amphiphilic block copolymers, in an aqueous milieu. NK012 was obtained as a freeze-dried formulation and contained ca. 20% (w/w) of SN-38 (Fig. 1). The mean particle size of NK012 is 20 nm in diameter with a relatively narrow range. The percentage released of SN-38 from NK012 in phosphate buffered saline at 37 °C were 57% and 74% at 24 h and 48 h, respectively, and that in 5% glucose solution at 37 °C were 1% and 3% at 24 h and 48 h, respectively. These results indicate that NK012 can release SN-38 under neutral condition even without the presence of a hydrolytic enzyme, and is stable in 5% glucose solution. In the formulation of NK012, SN-38 is bound to carboxyl group of hydrophobic chain of the block copolymer via ester bond and hydrolyzed to release SN-38. This ester bond may be cut gradually but efficiently at weak basic condition (PBS, pH 7.4) but very stable at weak acidic condition (5% glucose, pH 4.0). Consequently, it is suggested that NK012 is stable before administration and starts to release SN-38, the active component, inside a tumor following the accumulation of micelles into tumor tissue by utilizing the EPR effect.

3. Preclinical studies

3.1. Pancreatic cancer

Human pancreatic cancer is well known to have the worst prognosis [16]. At the time of diagnosis, the vast majority of the cancer extends beyond the pancreas. Direct invasion to nearby organs such as the stomach, duodenum, colon, spleen, and kidney is common. Distant metastasis to the liver and peritoneal dissemination are also common [17,18]. Gemcitabine is a first-line therapy for patients with advanced pancreatic cancer; however, only a response rate within 6–11% was

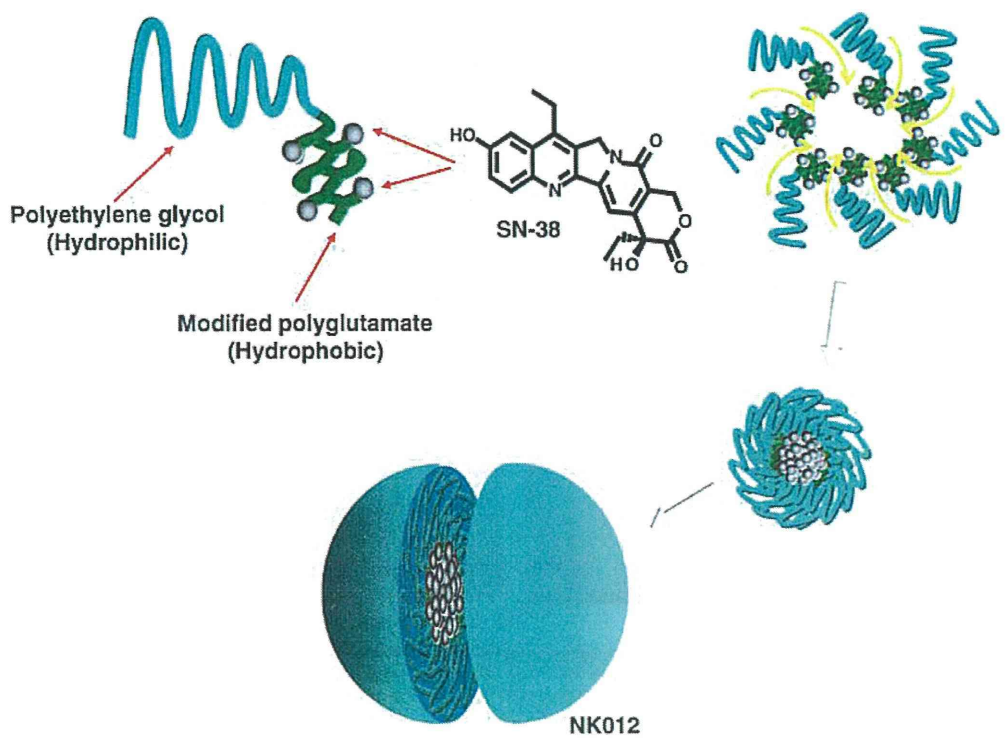

Fig. 1. Schematic structure of NK012. A polymeric micelle carrier of NK012 consists of a block copolymer of PEG (molecular weight of about Mw. 12,000 Da) and partially modified polyglutamate (about 20 units). Polyethylene glycol (hydrophilic) is believed to be the outer shell and SN-38 was incorporated into the inner core of the micelle.

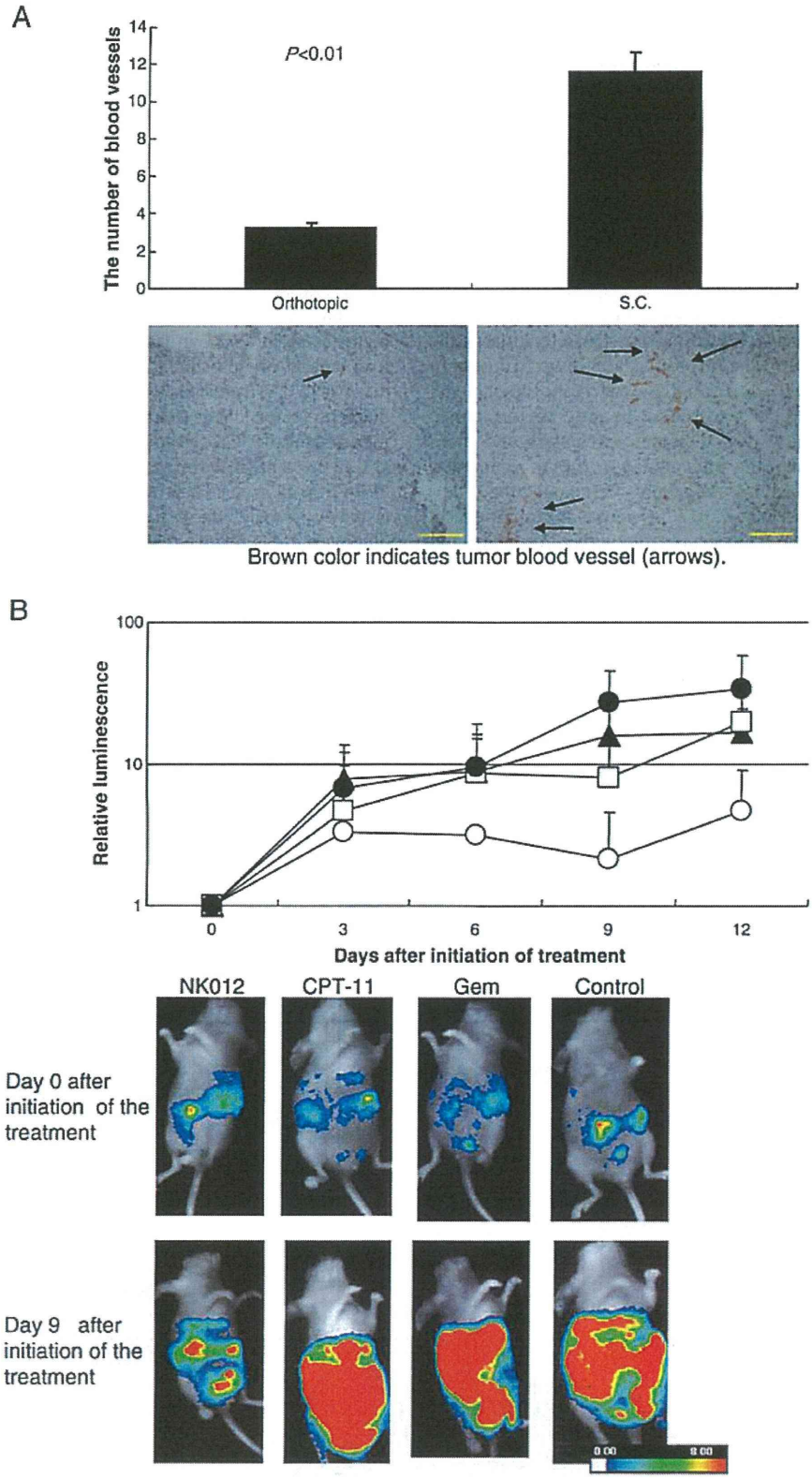

Fig. 2. (A) Number of blood vessels in orthotopic SUIT-2 tumor xenografts and subcutaneous (S.C.) tumor xenografts. After immunostaining with anti-factor VIII antibody, the number of tumor blood vessels (arrows) in each xenograft was counted. Column, mean + SD. $P<0.01$ (orthotopic vs S.C.). Scale bar: 200 μm. (B) Antitumor effects of NK012 in orthotopic tumor xenografts. Mice bearing SUIT-2 tumors were assigned into 4 groups 21 days after tumor inoculation. Mice were intravenously administered with NK012 (○) (30 mg/kg/day), CPT-11 (▲) (66.7 mg/kg/day), and 0.9% NaCl solution (●) (as a control) on days 0 (21 days after tumor inoculation), 4, and 8. Gemcitabine (□) (16.5 mg/kg/day) was administrated intraperitoneally on days 0, 3, 6, and 9. Representative luminescence intensity images obtained in individual control and treatment group mice on days 0 and 9. Points, mean + SD. $P=0.0074$ (NK012 vs control), $P=0.0231$ (NK012 vs CPT-11), $P=0.0239$ (NK012 vs gemcitabine).

observed in pancreatic cancer patients treated with gemcitabine [19,20]. The recent success of molecular-targeting agents has some impact on pancreatic cancer treatment. A recent phase III trial of gemcitabine alone vs gemcitabine and erlotinib (a tyrosine kinase inhibitor) in patients with advanced pancreatic cancer showed that overall survival was significantly improved with gemcitabine and erlotinib compared with gemcitabine and placebo. However, the improvement in median overall survival with gemcitabine and erlotinib was modest (6.24 months vs 5.91 months) [21]. Therefore, novel therapeutic approaches against invasive advanced pancreatic cancer are urgently needed. There are several reasons why pancreatic cancer is intractable clinically. One is that anticancer drugs are not efficiently and sufficiently delivered to the cancer cells within pancreatic cancer tissues. This is because human pancreatic cancer is hypovascular [22,23] and is rich in interstitial tissue, which may hinder efficient distribution of anticancer drugs to the entire pancreatic cancer tissue. We used an orthotopic pancreatic tumor model to evaluate the antitumor effects of NK012 because the orthotopic pancreatic cancer xenografts showed poorer vasculature and more abundant interstitium than the subcutaneous tumor xenografts (Fig. 2A). Moreover, peritoneal dissemination accompanied the orthotopic tumor. We have shown that NK012 has potent antitumor effects against orthotopic pancreatic tumors compared with gemcitabine and CPT-11, and that NK012 decreased the number of metastatic nodules in the peritoneal cavity (Fig. 2B). Thus, we admonish that it is better to use orthotopic tumor xenografts to evaluate antitumor activity against cancer characterized by few tumor vessels and high amount of tumor stroma. Moreover, enhanced accumulation, distribution, and retention of polymeric micelle-based anticancer drugs within the tumor tissue and the sustained release of anticancer drugs from the micelles are key elements for the treatment of hypovascular tumors [24].

3.2. Lung cancer

The median survival of small cell lung cancer (SCLC) patients treated with the CPT-11/cisplatin (cis-dichlorodiammineplatinum (II): CDDP) combination was significantly longer than that of SCLC patients treated with the etoposide/CDDP combination in a randomized phase III study conducted by the Japanese Cooperative Oncology Group (JCOG) [25]. Therefore, CPT-11/CDDP is considered to be one of the most active regimens against SCLC in Japan. One of the major clinically important toxic effects or dose limiting factors of CPT-11 is severe late-onset diarrhea [26]. We previously demonstrated that there was no significant difference in the kinetic character of free SN-38 in the small intestine of mice bearing the SCLC cell line SBC-3 and treated with NK012 and CPT-11 [13]. In this context, we investigated the advantages of NK012/CDDP over CPT-11/CDDP in mice bearing a SCLC xenograft in terms of antitumor activity and toxic effects, particularly intestinal toxicity. A significant difference in the relative tumor volume on day 30 was found between NK012/CDDP and CPT-11/CDDP treatments. Inflammatory changes in the small intestinal mucosa were rare in all NK012-treated mice, but were commonly observed in CPT-11-treated mice (Fig. 3). Moreover, a large amount of CPT-11 was excreted into the feces and high CPT-11

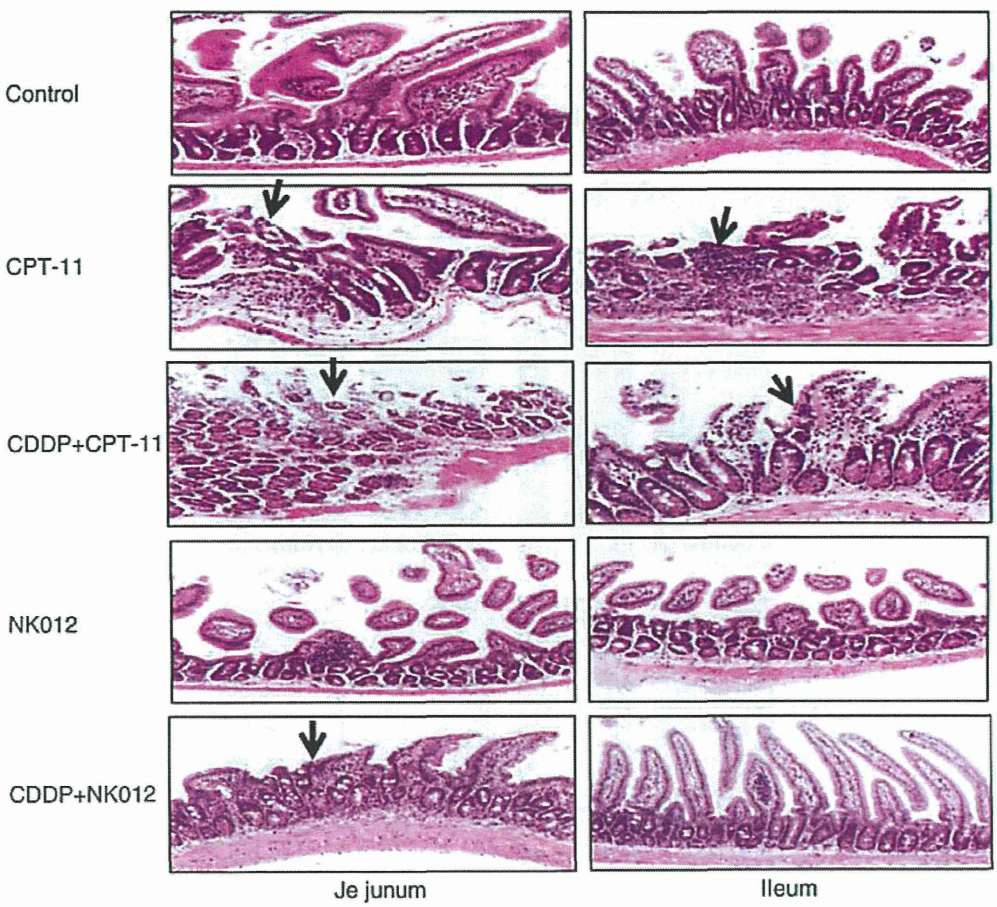

Fig. 3. Pathological findings and characteristic mucosal changes (arrows) in mouse. CPT-11 treatment group: healed erosion with fibrotic changes and lymphocytic invasion in the jejuna mucosa. Severe glandular arrangement. Active inflammation with inflammatory cell invasion and disappearance of gland ducts on the ileal mucosa. CPT-11/CDDP treatment group: healed erosion with scar-like fibrotic growth in the jejuna mucosa and mild inflammatory cell invasion into the ileal mucosa. NK012, NK012/CDDP treatment group and control: no inflammatory changes in the ileal mucosa. Mild shortening and decreased number of villi or mild inflammatory cell invasion in the jejuna mucosa in the NK012/CDDP treatment group.